

# MODELLING, SIMULATION AND IMPLEMENTATION OF AUTONOMOUS UNMANNED QUADROTOR

Yaser Alaiwi<sup>1</sup>, Aşkın Mutlu<sup>1</sup>

Faculty of Engineering – Department of Mechanical Engineering, Istanbul University Cerrahpaşa, Turkey<sup>1</sup>  
yaser.alaiwi@istanbul.edu.tr, askin@istanbul.edu.tr

**Abstract:** This research proposes modelling, simulation and implementation of autonomous unmanned quadrotor prototype based on Matlab Simulink software, and Mission Planner for communicating with APM control board of the quadrotor. The goal is to Control attitude and altitude over a desired trajectory of the Quadrotor using PID control, with high precision and reliability. The mathematical model used for simulation takes into account all differential equations of motion of the quadrotor. A full quadrotor prototype was assembled for real experiments to do a comparison between real and simulated data. This comparison reveals the reliability and the accuracy of the PID controller and the mathematical model used in Matlab.

**KEYWORDS:** QUADROTOR, UAV, SIMULATION, PID CONTROL, TRAJECTORY TRACKING.

## 1. Introduction

The Unmanned Aerial Vehicles (UAVs), particularly the Vertical Take-Off and Landing (VTOL) Quadrotors, are flying robots without pilot which are able to conduct missions in hostile and disturbed environments[1]. The rotors are directed upwards and they are placed in a square formation with equal distance from the center of mass of the quadrotor. The quadrotor is controlled by adjusting the angular velocities of the rotors which are spun by electric motors. Quadrotor is a typical design for small unmanned aerial vehicles (UAV) as shown in Figure 1. And because of the simple structure, Quadrotors are used in surveillance, search and rescue, construction inspections and several other applications.

Quadrotor has received a big attention from researchers as this new technology has generated several areas of interest. The basic dynamical model of the quadrotor is the starting point for all of the studies. Different control methods have been investigated, including PID controllers [2]–[5], Backstepping control method [6], [7], [8], LQR controllers [5], nonlinear  $H_\infty$  control and nonlinear controllers with nested saturations [9], [10]. but more complex aerodynamic properties has been introduced as well [11], [12]. Control methods require accurate measurement from the position and attitude sensors represented in a gyroscope, an accelerometer, and other measurement devices, such as GPS, sonar and laser sensors [13], [14].



Figure 1: Aeryon Skyranger Quadrotor.

The purpose of this research is to present the basics of quadrotor modelling and control as to form a basis for further research and development in the area. This is pursued with the first aim to study the mathematical model of the quadrotor dynamics and modelling it in Matlab to develop proper methods for trajectory tracking control of the quadrotor. The challenge in controlling a quadrotor is that the quadrotor has six degrees of freedom but there are only four control inputs which means an under-actuated system.

In this literature review we will show the differential equations of motion for a quadrotor, which could be derived from Newton-Euler and Euler-Lagrange equations. The behavior of the model is examined by simulating the flight of the quadrotor. Stabilization of the quadrotor is conducted by utilizing a PID controller. The PID control method is easy to implement and to be used for the quadrotor control.

## 2. Dynamic System Model

The quadrotor structure is presented in Figure 2 including the corresponding angular velocities, torques and forces created by the four rotors (numbered from 1 to 4).

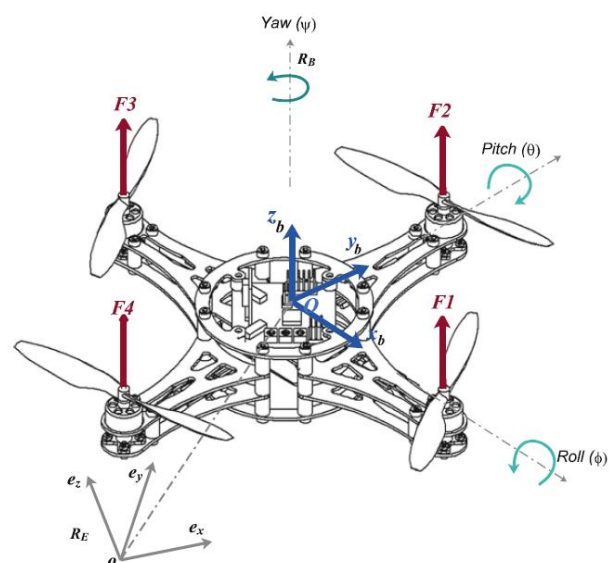


Figure 2: The inertial and body frames of a quadrotor.

The absolute linear position of the quadrotor is defined in the inertial frame  $x, y, z$  axes with  $\xi$ . The attitude, i.e. the angular position, is defined in the inertial frame with three

Euler angles  $\eta$ . Pitch angle  $\theta$  determines the rotation of the quadrotor around the y-axis. Roll angle  $\phi$  determines the rotation around the x-axis and yaw angle  $\psi$  around the z-axis. Vector  $q$  contains the linear and angular position vectors:

$$\xi = \begin{bmatrix} x \\ y \\ z \end{bmatrix}, \quad \eta = \begin{bmatrix} \phi \\ \theta \\ \psi \end{bmatrix}, \quad q = \begin{bmatrix} \xi \\ \eta \end{bmatrix} \quad (1)$$

The origin of the body frame is in the center of mass of the quadrotor. The linear velocities in the body frame are determined by  $V_B$  and the angular velocities by  $v$ :

$$V_B = \begin{bmatrix} v_{x,B} \\ v_{y,B} \\ v_{z,B} \end{bmatrix}, \quad v = \begin{bmatrix} p \\ q \\ r \end{bmatrix} \quad (2)$$

The rotation matrix from the body frame to the inertial frame is:

$$R = \begin{bmatrix} C_\psi C_\theta & C_\psi S_\theta S_\phi - S_\psi C_\phi & C_\psi S_\theta C_\phi + S_\psi S_\phi \\ S_\psi C_\theta & S_\psi S_\theta S_\phi + C_\psi C_\phi & S_\psi S_\theta C_\phi - C_\psi S_\phi \\ -S_\theta & C_\theta S_\phi & C_\theta C_\phi \end{bmatrix} \quad (3)$$

In which  $S_x = \sin(x)$  and  $C_x = \cos(x)$ . The rotation matrix  $R$  is orthogonal thus  $R^{-1} = R^T$  which is the rotation matrix from the inertial frame to the body frame.

The transformation matrix for angular velocities from the inertial frame to the body frame is  $W_\eta$ , and from the body frame to the inertial frame is  $W_\eta^{-1}$ , is as shown:

$$\dot{\eta} = W_\eta^{-1} v, \quad \begin{bmatrix} \dot{\phi} \\ \dot{\theta} \\ \dot{\psi} \end{bmatrix} = \begin{bmatrix} 1 & S_\phi T_\theta & C_\phi T_\theta \\ 0 & C_\phi & -S_\phi \\ 0 & S_\phi / C_\theta & C_\phi / C_\theta \end{bmatrix} \begin{bmatrix} p \\ q \\ r \end{bmatrix},$$

$$v = W_\eta \dot{\eta}, \quad \begin{bmatrix} p \\ q \\ r \end{bmatrix} = \begin{bmatrix} 1 & 0 & -S_\theta \\ 0 & C_\phi & C_\theta S_\phi \\ 0 & -S_\phi & C_\theta C_\phi \end{bmatrix} \begin{bmatrix} \dot{\phi} \\ \dot{\theta} \\ \dot{\psi} \end{bmatrix} \quad (4)$$

In which  $T_x = \tan(x)$ . The matrix  $W_\eta$  is invertible if  $\theta \neq (2k - 1) \pi / 2, (k \in \mathbb{Z})$ .

The quadrotor is assumed to have symmetric structure with the four arms aligned with the body x- and y-axes. Thus, the inertia matrix is diagonal matrix  $I$  in which  $I_{xx} = I_{yy}$

$$I = \begin{bmatrix} I_{xx} & 0 & 0 \\ 0 & I_{yy} & 0 \\ 0 & 0 & I_{zz} \end{bmatrix} \quad (5)$$

The angular velocity of rotor  $i$ , denoted with  $\omega_i$ , creates force  $f_i$  in the direction of the rotor axis. The angular velocity and acceleration of the rotor also create torque  $\tau_{M_i}$  around the rotor axis

$$f_i = k\omega_i^2, \quad \tau_{M_i} = b\omega_i^2 + I_M \dot{\omega}_i, \quad (6)$$

Here is the lift constant  $k$ , the drag constant  $b$  and the inertia moment of the rotor is  $I_M$ . generally, the effect of  $\dot{\omega}_i$  is considered small, so it is omitted.

The combined forces of rotors create thrust force  $T$  in the direction of the body z-axis. Torque  $\tau_B$  consists of the torques  $\tau_\phi, \tau_\theta$  and  $\tau_\psi$  in the direction of the corresponding body frame angles

$$T = \sum_{i=1}^4 f_i = k \sum_{i=1}^4 \omega_i^2, \quad T^B = \begin{bmatrix} 0 \\ 0 \\ T \end{bmatrix} \quad (7)$$

$$T_B = \begin{bmatrix} T_\phi \\ T_\theta \\ T_\psi \end{bmatrix} = \begin{bmatrix} lk(-\omega_2^2 + \omega_4^2) \\ lk(-\omega_1^2 + \omega_3^2) \\ k \sum_{i=1}^4 \tau_{M_i} \end{bmatrix} \quad (8)$$

Here  $l$  is the distance between the rotor center and the center of mass of the quadrotor. Thus, the roll movement is acquired by decreasing the 2<sup>nd</sup> rotor velocity and increasing the 4<sup>th</sup> rotor velocity. In the same way, the pitch movement is acquired by decreasing the 1<sup>st</sup> rotor velocity and increasing the 3<sup>rd</sup> rotor velocity. Yaw movement is acquired by increasing the angular velocities of two opposite rotors and decreasing the velocities of the other two.

### 3. Euler-Lagrange equations of motion:

The Lagrangian  $L$  is the sum of the translational  $E_{trans}$  and rotational  $E_{rot}$  energies minus potential energy  $E_{pot}$

$$\mathcal{L}(q, \dot{q}) = E_{trans} + E_{rot} - E_{pot} = (m/2)\dot{\xi}^T \dot{\xi} + (1/2)v^T I v - mgz. \quad (9)$$

Equations of external forces and torques are:

$$\begin{bmatrix} f \\ \tau \end{bmatrix} = \frac{d}{dt} \left( \frac{\partial \mathcal{L}}{\partial \dot{q}} \right) - \frac{\partial \mathcal{L}}{\partial q} \quad (10)$$

The linear and angular components do not depend on each other thus they can be studied separately. The linear external force is the total thrust of the rotors. The linear Euler-Lagrange equations are

$$f = RT_B = m\ddot{\xi} + mg \begin{bmatrix} 0 \\ 0 \\ 1 \end{bmatrix}, \quad (11)$$

$$\begin{bmatrix} \ddot{x} \\ \ddot{y} \\ \ddot{z} \end{bmatrix} = -g \begin{bmatrix} 0 \\ 0 \\ 1 \end{bmatrix} + \frac{T}{m} \begin{bmatrix} C_\psi S_\theta C_\phi + S_\psi S_\phi \\ S_\psi S_\theta C_\phi - C_\psi S_\phi \\ C_\theta C_\phi \end{bmatrix}$$

$$\ddot{x} = \frac{1}{m} (c\phi c\psi s\theta + s\phi s\psi) u_1$$

$$\ddot{y} = \frac{1}{m} (c\phi s\psi s\theta - s\phi c\psi) u_1$$

$$\ddot{z} = \frac{1}{m} c\phi c\theta u_1 - g$$

The Jacobian matrix  $J(\eta)$  [15] from  $v$  to  $\dot{\eta}$  is:

$$J(\eta) = J = W_\eta^T I W_\eta, \quad (12)$$

$$J(\eta) = \begin{bmatrix} I_{xx} & 0 & -I_{xx} S_\theta \\ 0 & I_{yy} C_\phi^2 + I_{zz} S_\phi^2 & (I_{yy} - I_{zz}) C_\phi S_\phi C_\theta \\ -I_{xx} S_\theta & (I_{yy} - I_{zz}) C_\phi S_\phi C_\theta & I_{xx} S_\theta^2 + I_{yy} S_\phi^2 C_\theta^2 + I_{zz} C_\phi^2 C_\theta^2 \end{bmatrix}$$

Thus, the rotational energy  $E_{rot}$  can be expressed in the inertial frame as:

$$E_{rot} = (1/2)v^T I v = (1/2)\dot{\eta}^T J \dot{\eta} \quad (13)$$

The external angular force is the torques of the rotors [16]. The angular Euler-Lagrange equations are

$$\tau = \tau_B = J\ddot{\eta} + \frac{d}{dt} (J\dot{\eta}) - \frac{1}{2} \frac{\partial}{\partial \eta} (\dot{\eta}^T J \dot{\eta}) = J\ddot{\eta} + C(\eta, \dot{\eta})\dot{\eta} \quad (14)$$

in which the matrix  $C(\eta, \dot{\eta})$  is the Coriolis term, containing the gyroscopic and centripetal terms. The matrix  $C(\eta, \dot{\eta})$  has the form, as shown in [8],

$$C(\eta, \dot{\eta}) = \begin{bmatrix} C_{11} & C_{12} & C_{13} \\ C_{21} & C_{22} & C_{23} \\ C_{31} & C_{32} & C_{33} \end{bmatrix}$$

$$\begin{aligned} C_{11} &= 0 \\ C_{12} &= (I_{yy} - I_{zz})(\dot{\theta}C_{\phi}C_{\theta} + \dot{\psi}S_{\phi}^2C_{\theta}) + (I_{zz} - I_{yy})\dot{\psi}C_{\phi}^2C_{\theta} - I_{xx}\dot{\psi}C_{\theta} \\ C_{13} &= (I_{zz} - I_{yy})\dot{\psi}C_{\phi}S_{\phi}C_{\theta}^2 \\ C_{21} &= (I_{zz} - I_{yy})(\dot{\theta}C_{\phi}S_{\phi} + \dot{\psi}S_{\phi}C_{\theta}) + (I_{yy} - I_{zz})\dot{\psi}C_{\phi}^2C_{\theta} + I_{xx}\dot{\psi}C_{\theta} \\ C_{22} &= (I_{zz} - I_{yy})\dot{\phi}C_{\phi}S_{\phi} \\ C_{23} &= -I_{xx}\dot{\psi}S_{\theta}C_{\theta} + I_{yy}\dot{\psi}S_{\phi}^2S_{\theta}C_{\theta} + I_{zz}\dot{\psi}C_{\phi}^2S_{\theta}C_{\theta} \\ C_{31} &= (I_{yy} - I_{zz})\dot{\psi}C_{\theta}^2S_{\phi}C_{\theta} - I_{xx}\dot{\theta}C_{\theta} \\ C_{32} &= (I_{zz} - I_{yy})(\dot{\theta}C_{\phi}S_{\phi}S_{\theta} + \dot{\phi}S_{\phi}^2C_{\theta}) + (I_{yy} - I_{zz})\dot{\phi}C_{\phi}^2C_{\theta} \\ &\quad + I_{xx}\dot{\psi}S_{\theta}C_{\theta} - I_{yy}\dot{\psi}S_{\phi}^2S_{\theta}C_{\theta} - I_{zz}\dot{\psi}C_{\phi}^2S_{\theta}C_{\theta} \\ C_{33} &= (I_{yy} - I_{zz})\dot{\phi}C_{\phi}S_{\phi}C_{\theta}^2 - I_{yy}\dot{\theta}S_{\phi}^2C_{\theta}S_{\theta} - I_{zz}\dot{\theta}C_{\phi}^2C_{\theta}S_{\theta} + I_{xx}\dot{\theta}C_{\theta}S_{\theta} \end{aligned}$$

Equation (14) leads to the differential equations for the angular accelerations:

$$\ddot{\eta} = J^{-1}(\tau_B - C(\eta, \dot{\eta})\dot{\eta}) \tag{16}$$

$$\begin{aligned} \ddot{\phi} &= \frac{I_y - I_z}{I_x} \dot{\theta} \dot{\psi} - \frac{J_r}{I_x} \Omega_r \dot{\theta} + \frac{1}{I_x} u_2 \\ \ddot{\theta} &= \frac{I_z - I_x}{I_y} \dot{\phi} \dot{\psi} - \frac{J_r}{I_y} \Omega_r \dot{\phi} + \frac{1}{I_y} u_3 \\ \ddot{\psi} &= \frac{I_x - I_y}{I_z} \dot{\theta} \dot{\phi} + \frac{1}{I_z} u_4 \end{aligned}$$

From (15) and (16) we can find the equations of motion for translational and rotational movement of the quadrotor system.

The influence of aerodynamical effects are complicated and difficult to model. Also it has significant effect only in high velocities. Thus, these effects are excluded from the model and a simplified model is used.

#### 4. Controller Design:

To stabilize the quadrotor, a PID controller is utilized. Advantages of the PID controller are easy implementation and tuning of the controller. The known form of the PID controller is as follows:

$$u(t) = K_P e(t) + K_I \int_0^t e(\tau) d\tau + K_D \frac{de(t)}{dt} \tag{17}$$

in which  $u(t)$  is the control input,  $e(t)$  is the difference between the desired state  $x_d(t)$  and the present state  $x(t)$ , and  $K_P$ ,  $K_I$  and  $K_D$  are the parameters for the proportional, integral and derivative elements of the PID controller.

In a quadrotor, there are six states, positions  $\xi$  and angles  $\eta$ , but only four control inputs, the angular velocities of the four rotors  $\omega_i$ . The interactions between the states and the total thrust  $T$  and the torques  $\tau$  created by the rotors are clear as we can see in the dynamical equations of motion. The total thrust  $T$  affects the acceleration in the direction of the z-axis and holds the quadrotor in the air. Torque  $\tau_{\phi}$  has an effect on the acceleration of angle  $\phi$ , torque  $\tau_{\theta}$  affects the acceleration

of angle  $\theta$ , and torque  $\tau_{\psi}$  contributes in the acceleration of angle  $\psi$ .

The role of the PID controller is to adjust the speed of the four motors thus propellers such that a desired quadrotor orientation is achieved. The Quadrotor is controlled by independently varying the speed of the four rotors. Hence, these control inputs  $u^{-1,2,3,4}$  are defined as follows:

$$u = \begin{bmatrix} u_1 \\ u_2 \\ u_3 \\ u_4 \end{bmatrix} = \begin{bmatrix} F \\ \tau_{\phi} \\ \tau_{\theta} \\ \tau_{\psi} \end{bmatrix} = \begin{bmatrix} b & b & b & b \\ 0 & -lb & 0 & lb \\ -lb & 0 & lb & 0 \\ d & -d & d & -d \end{bmatrix} \begin{bmatrix} \omega_1^2 \\ \omega_2^2 \\ \omega_3^2 \\ \omega_4^2 \end{bmatrix} \tag{18}$$

$$\begin{pmatrix} u_1 \\ u_2 \\ u_3 \\ u_4 \end{pmatrix} = \begin{pmatrix} b(\omega_1^2 + \omega_2^2 + \omega_3^2 + \omega_4^2) \\ b(-\omega_2^2 + \omega_4^2) \\ b(\omega_1^2 - \omega_3^2) \\ d(\omega_1^2 - \omega_2^2 + \omega_3^2 - \omega_4^2) \end{pmatrix} \tag{19}$$

$$\omega_1^2 = \frac{u_1}{4b} - \frac{u_3}{2lb} + \frac{u_4}{4d}$$

$$\omega_2^2 = \frac{u_1}{4b} + \frac{u_3}{2lb} - \frac{u_4}{4d}$$

$$\omega_3^2 = \frac{u_1}{4b} + \frac{u_3}{2lb} + \frac{u_4}{4d}$$

$$\omega_4^2 = \frac{u_1}{4b} - \frac{u_3}{2lb} - \frac{u_4}{4d}$$

(20)

#### 4.1 Description of the Simulation Tool:

We built the Simulink block diagram for the quadrotor dynamics as shown in Figure 3. Which represent the translational and rotational system dynamics, also we can see special block for motor speed calculation.

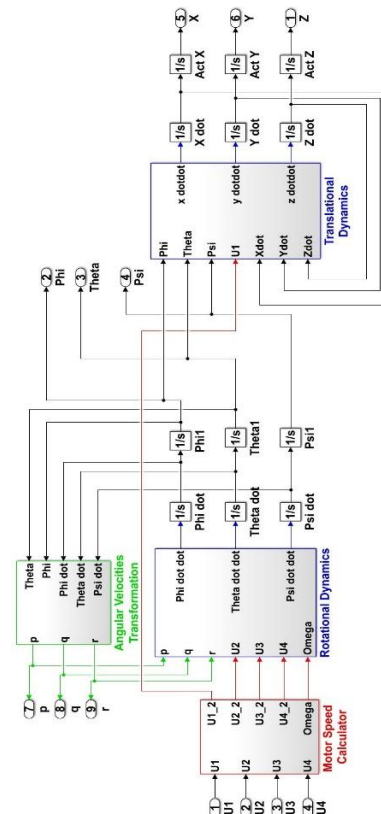


Figure 3: Quadrotor Dynamics diagram in Simulink

The Full system with controller and trajectory generator can be seen in Figure 4.

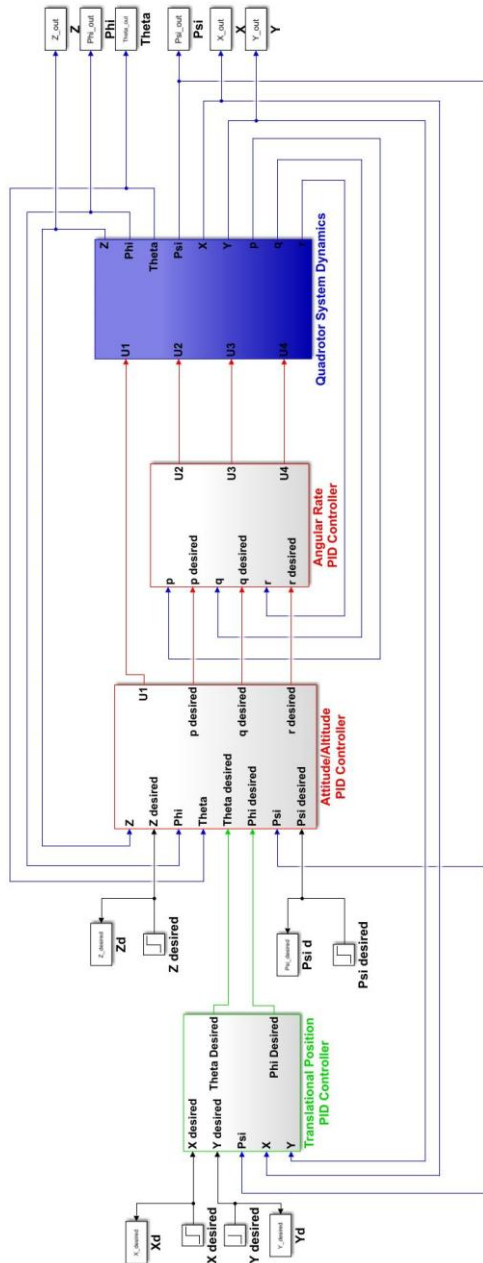


Figure 4: Simulink Diagram with PID controllers

Quadrotor controller is implemented using nested control loops. The inner most loop controls the angular velocities of the quadrotor. This loop needs to run at a high frequency due to the fast dynamics of the quadrotor. The next highest loop controls the attitude and altitude of the quadrotor. Small attitude changes are directly related to translational acceleration. This means small attitude errors can cause large and unwanted translational displacements very quickly.

Small attitude angles will result in translational movement or drifting of the quadrotor. In order to prevent this translational drifting behavior, a position controller is implemented.

**5. Implementation and Design:**

Quadrotor implementation and selecting the correct parts is a very important step. Because we should calculate the total weight of the quadrotor and according to that the suitable parts will be selected. Our quadrotor weight is 1.3 kg. we used APM 2.6 ArduPilot Mega 2.6 Flight Control Board as shown in Figure 5. The Ardupilot is connected to ESCs for

controlling the four motors speed. We selected DJI F450 frame and 10 inch propellers. FlySky 9 channels remote control is used for sending control signals and communicating with APM control board.

On the ground station we used Ardupilot mission planner software and by using 900 MHz telemetry device we could communicate with quadrotor. Figure 5 shows Communication process between the different parts of the quadrotor.



Figure 5: Communication process between quadrotor different parts.

After that we built the real model of the quadrotor by assembling all the parts together in one unit. Then we uploaded the open source of the ArduPilot to the control card, and by finishing the motor tests and ESCs calibrations we could make the real flight experiments.

We can see the full model of the quadrotor in Figure 6 whereas the upper black part is the GPS device used for locating the position. While the IMU (Inertial measurement unit) is used for measuring angular speeds and acceleration of the quadrotor.



Figure 6: Quadrotor Full Model Assembly.

The flight experiments were done at Istanbul university campus. We made manual and autonomous flight tests, and we could send the trajectories from the ground station to the control board over the quadrotor to be tracked automatically.

The manual tests done to assure the consistency and compatibility of the quadrotor parts with each other. Some photos were taken while doing tests as shown in figure 7.



Figure 7: Trajectory tracking and Flight test at Istanbul university campus.

6. Simulation Results:

The model was verified by simulating the flight of a quadrotor within Matlab. Blocks that representing all external forces, torques and loads acting on the model have been integrated into the block diagrams model. Then we generated the desired 3D trajectories to follow it using the Mission Planner open source software. This simulator is able to predict the latitude and altitude on the desired trajectory in order to represent real model with high reliability as shown in Figure 8 and Figure 9.

Stabilization of attitude of the quadrotor was done by utilizing a PID controller. The simulation proved the presented mathematical model to be realistic in modelling the position and attitude of the quadrotor.

Finally, the required control inputs were solved from the total thrust and the torques. The simulation results indicated that the quadrotor could be controlled accurately with the control inputs given from the computer throw telemetry to the quadrotor.

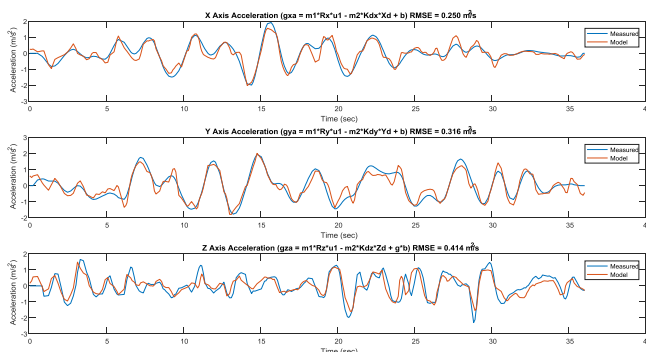


Figure 8: Measured and modeled acceleration control Plots.

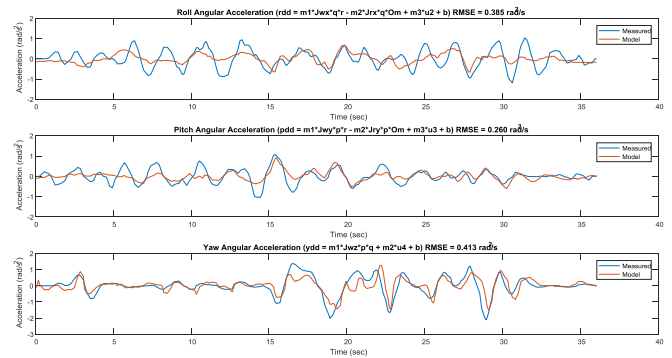


Figure 9: Measured and modeled roll control plots.

For 10 seconds period of simulation time we can see the measured and desired Roll angle in figure 10. Also measured accelerations over x, y and z could be seen in figure 11.

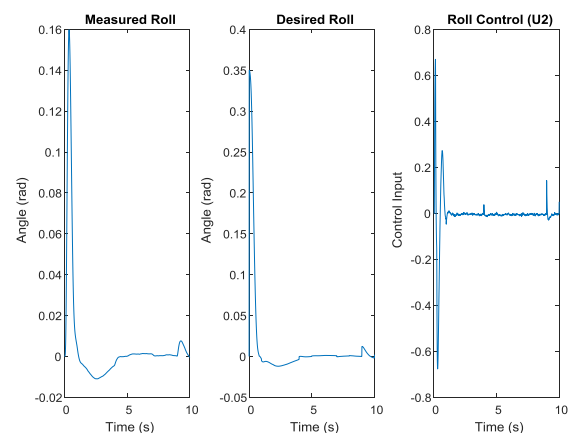


Figure 10: Roll Control plots.

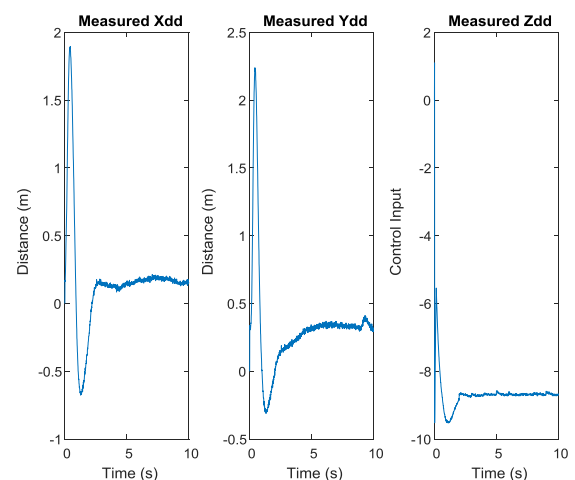


Figure 11: Acceleration Control Plots.

7. Conclusion

This research studied mathematical modelling and control of a quadrotor system as well as the implementation of the Quadrotor real model using Simulink® for mathematical modelling and simulation of the differential equations of motion of a quadrotor. The mathematical model of quadrotor dynamics was presented and the differential equations of motion were derived from the Euler-Lagrange equations.

The presented mathematical model only consists of the basic structures of the quadrotor dynamics. Several aero dynamical

effects were excluded which can lead to unrealizable behavior. The position and attitude information was assumed to be accurate in the model and the simulations. However, the measuring devices in real life are not perfectly accurate as random variations and errors occur. Hence, the effects of imprecise information to the flight of the quadrotor should be studied as well. Also there are methods to enhance the accuracy of the measurements which should be researched and implemented to improve all aspects required for robust quadrotor maneuvers.

The presented model and control methods were tested both in simulations and Real experimental prototype of a quadrotor that constructed to achieve more realistic and reliable results. With a real prototype, the theoretical framework and the simulation results could be compared to real-life measurements.

Finally, simulation results indicate that the applied PID controller over ArduPilot control board can follow the desired trajectory with high precision. Block parameters used for defining the model can be easily modified to be adapted to other assembly models. Moreover, the model can be used to simulate any other quadrotor with different parameters and to predict the resultant errors.

## References

- [1] S. V. C. Lien, *Applications of Sliding Mode Control in Science and Engineering*, vol. 709. 2017.
- [2] İ. C. Dikmen, A. Arisoy, and H. Temeltas, "Attitude control of a quadrotor," in *Recent Advances in Space Technologies, 2009. RAST'09. 4th International Conference on*, 2009, pp. 722–727.
- [3] A. Tayebi and S. McGilvray, "Attitude stabilization of a four-rotor aerial robot," in *Decision and Control, 2004. CDC. 43rd IEEE Conference on*, 2004, vol. 2, pp. 1216–1221.
- [4] Z. Zuo, "Trajectory tracking control design with command-filtered compensation for a quadrotor," *IET Control theory Appl.*, vol. 4, no. 11, pp. 2343–2355, 2010.
- [5] S. Bouabdallah, A. Noth, and R. Siegwart, "PID vs LQ control techniques applied to an indoor micro quadrotor," in *Intelligent Robots and Systems, 2004.(IROS 2004). Proceedings. 2004 IEEE/RSJ International Conference on*, 2004, vol. 3, pp. 2451–2456.
- [6] T. Madani and A. Benallegue, "Backstepping Control for a Quadrotor Helicopter."
- [7] K. M. Zemalache, L. Beji, and H. Marref, "Control of an under-actuated system: application a four rotors rotorcraft," in *Robotics and Biomimetics (ROBIO). 2005 IEEE International Conference on*, 2005, pp. 404–409.
- [8] G. V. Raffo, M. G. Ortega, and F. R. Rubio, "An integral predictive/nonlinear  $H_\infty$  control structure for a quadrotor helicopter," *Automatica*, vol. 46, no. 1, pp. 29–39, 2010.
- [9] P. Castillo, R. Lozano, and A. Dzul, "Stabilization of a mini rotorcraft with four rotors," *IEEE Control Syst.*, vol. 25, no. 6, pp. 45–55, 2005.
- [10] J. Escareno, S. Salazar-Cruz, and R. Lozano, "Embedded control of a four-rotor UAV," in *American Control Conference, 2006, 2006*, p. 6 pp.
- [11] G. Hoffmann, H. Huang, S. Waslander, and C. Tomlin, "Quadrotor helicopter flight dynamics and control: Theory and experiment," in *AIAA Guidance, Navigation and Control Conference and Exhibit*, 2007, p. 6461.
- [12] H. Huang, G. M. Hoffmann, S. L. Waslander, and C. J. Tomlin, "Aerodynamics and control of autonomous quadrotor helicopters in aggressive maneuvering," in *Robotics and Automation, 2009. ICRA'09. IEEE International Conference on*, 2009, pp. 3277–3282.
- [13] P. Martin and E. Salaün, "The true role of accelerometer feedback in quadrotor control," in *Robotics and Automation (ICRA), 2010 IEEE International Conference on*, 2010, pp. 1623–1629.
- [14] R. He, S. Prentice, and N. Roy, "Planning in information space for a quadrotor helicopter in a GPS-denied environment," in *Robotics and Automation, 2008. ICRA 2008. IEEE International Conference on*, 2008, pp. 1814–1820.
- [15] C. K. Tan, J. Wang, Y. C. Paw, and T. Y. Ng, "Tracking of a moving ground target by a quadrotor using a backstepping approach based on a full state cascaded dynamics," *Appl. Soft Comput. J.*, vol. 47, pp. 47–62, 2016.
- [16] D. Mercado, P. Castillo, R. Castro, and R. Lozano, "2-sliding mode trajectory tracking control and EKF estimation for quadrotors," in *IFAC Proceedings Volumes (IFAC-PapersOnline)*, 2014.